Geiger tube, parallel to the face of the specimen. Such a photogram indicates the intensity of diffraction over the radiated area. A pair of such pictures taken at 25 seconds of arc apart with the entire face irradiated is shown in Fig. 2. These indicate that the specimen consists of two highly perfect lattices rotated from one another about the growth axis. The sharpness with which the two regions are delineated in the x-ray photograms is particularly striking, since no boundary was visible in this face on microscopic examination, a fact which is in keeping with the directional nature of the dislocations.

The correlation of these observations and measurements with Burgers' model is consistent with the assumption that these lineage boundaries consist of edge dislocations whose sites are indicated by the etch pits.

The writers are indebted to W. L. Bond for the use of precision x-ray apparatus designed by him and to W. T. Read for helpful discussions.

[1] J. M. Burgers, Proc. Phys. Soc. (London) **52**, 23 (1940).
[2] P. LaCombe, *Report of Conference on Strength of Solids* (The Physical Society, London, 1948).
[3] W. T. Read and W. Shockley, Phys. Rev. **78**, 275 (1950).
[4] W. G. Pfann and K. M. Olsen, Phys. Rev. **89**, 322 (1953).

Electron Beam Interferometer*

L. MARTON, J. AROL SIMPSON, AND J. A. SUDDETH
National Bureau of Standards, Washington, D. C.
(Received March 2, 1953)

IN an earlier paper[1] the view was advanced that an interferometer operating with electron beams would be a useful instrument for many physical measurements. In the same paper reasons were given for concentrating on amplitude splitting (wide beam) type of instruments in preference to wave-front splitting (narrow beam) instruments. At the same time considerations were submitted for the use of electron diffraction on a lamellar single crystal as a beam splitting device.

For practical purposes the three-crystal arrangement of that earlier paper was chosen. The resulting beam trajectories make the instrument somewhat analogous to a very skew Mach-Zehnder light interferometer.

An instrument of this kind has been constructed consisting of three crystal mounts each of which can be rotated about the optical axis. This rotation is necessary for the orientation of crystals. The mount of the crystal, first in order of penetration of the electron beam, can also be translated along the axis to change the path difference. The fixed intercrystal distance is 3.48 cm. The crystals used have been prepared by the process known as epitaxy, and details of the techniques used are given elsewhere.[2,3] Although several metallic crystals were tried, such as gold, silver, nickel, and copper, copper was used for the final tests. The crystals are approximately 100A thick and about 3 mm in diameter. The interferometer vacuum chamber containing the three crystal mounts has been mounted on a conventional magnetic electron microscope replacing the object chamber of that instrument. In this manner the electron gun and condenser lens of the electron microscope serve as the necessary electron beam generating components, while the objective and projector lens of the instrument serve for viewing the interference fringes.

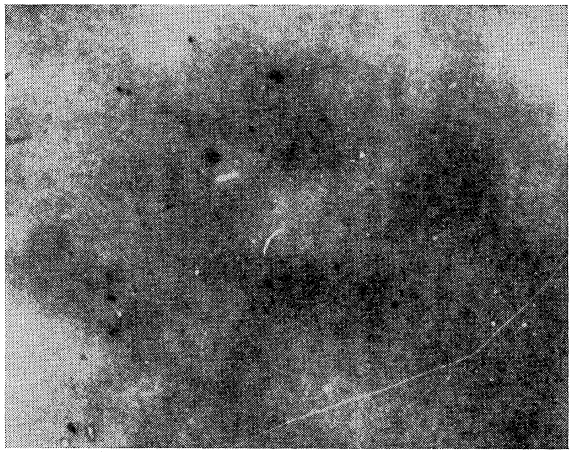

FIG. 1. Electron interference fringes superimposed on uneven crystal background. Total area shown—approximately $3\mu \times 4\mu$; average fringe spacing—1600A.

In the course of aligning and testing this instrument, two types of difficulties were encountered. One is due to the peculiarities of using diffraction as a beam-splitting mechanism. To achieve more familiarity with those peculiarities, it was found desirable to study more in detail its light optical analog using diffraction grating replicas in transmission. With this model, it was found that interferometers using diffraction both for beam splitting and beam deflection belong to an almost forgotten class of interferometers which are capable of forming a higher order fringe in a nonmonochromatic light.[4] This "achromatic" property is fortunate in that it relieves the stringent necessity for stability of power supplies over long exposures of the electron optical instrument. On the other hand, it has the disadvantage of limiting the application of the instrument to problems where the coherence properties of the source are of no interest. In other words, the instrument in its present form could not be used as an interferometric spectrometer for the study of electron emitters, whereas it could be used for wavelength determinations or field gradient studies. For the study of coherence phenomena, different interferometric arrangements would be necessary, the study of which is under way at present.

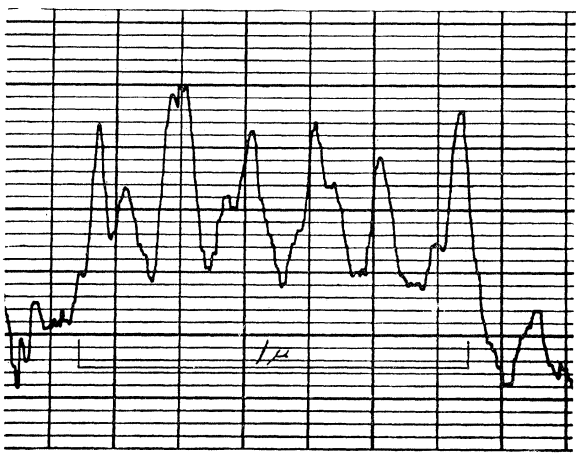

FIG. 2. Microphotometer tracing of some of the fringes shown in Fig. 1.

The second type of difficulty encountered in the operation of the instrument is due to a very low intensity. This low intensity is due to the loss of beam involved in using only a small part of the total beam diffracted at each of the three crystals. The initial intensity is limited by the small apertures of the objective lens and by the thermal destruction of the crystal and of the 50-μ mesh upon which the crystal is mounted. At the maximum beam intensity the electron optical parts could be operated to give a direct electron optical magnification of about 700 diameters. The resolving power of the instrument under these conditions is limited both by the electron optical system and by the grain of the photoplate to fringe spacings of the order of 1000A.

Figure 1 shows the appearance of a set of interference fringes

superimposed upon the much larger scale dark-field crystal pattern of the third crystal. Figure 2 shows a microdensitometer tracing of some of the fringes. To convince ourselves that these fringes were interference fringes due to the geometry of the instrument, this geometry has been slightly changed and the fringe behavior as a function of the changes investigated. It was found that within certain limitations a rotation of the third crystal by $2\frac{1}{2}°$ produced an 8° relative rotation of the fringes. The rotation of the fringes has been measured from a fixed direction on the crystal itself so that no ambiguity exists between fringe rotation and crystal rotation. We carried out some experiments changing the intercrystal distance between the first and second crystal and found that the fringe spacing varied as a function of that distance, as was to be expected.

The fringes to date are rather fugitive and hard to find, but it is believed that improved crystals will eliminate some of this difficulty.

A complete record of these experiments will be published at a later date.

* This investigation was conducted under a cooperative program of basic instrumentation research and development sponsored by the U. S. Office of Naval Research, the Air Research and Development Command, and the U. S. Atomic Energy Commission.

[1] L. Marton, Phys. Rev. **85**, 1057 (1952).
[2] O. G. Engel, J. Chem. Phys. **20**, 1174 (1952).
[3] O. G. Engel, J. Research Natl. Bur. Standards (to be published).
[4] C. Barus, Carnegie Institution of Washington Publication No. 149, Part I (1911), Part II (1912), Part III (1914).

Cyclotron Resonances, Magnetoresistance, and Brillouin Zones in Semiconductors

W. SHOCKLEY
Bell Telephone Laboratories, Murray Hill, New Jersey
(Received March 10, 1953)

ONE of the basic problems in the band theory of solids is to determine the shapes of the energy surfaces in the Brillouin zone. A possible solution is furnished by cyclotron resonances at low temperatures (say 10°K) in weakly doped germanium: For this situation, (1) Maxwell statistics can be used, (2) the interactions of the carriers are unimportant so that a description in terms of single carrier momenta in the Brillouin zone is good, and (3) the collision frequency ν is so much less than $\omega=2\pi f$ for 1.25-cm waves[1] that inertial effects dominate, and the dependence of ν upon position in the Brillouin zone is unimportant.

Some typical situations in which resonance might be observed are illustrated in Fig. 1. The E's and v's vary as $\exp(i\omega t)$ so that the conductivity $nq\mu$ is complex. The standard transverse and longitudinal magnetoresistance configurations are represented in (t) and (l), a combination of (t) and the Hall effect in (tH), and circular polarization in (c).

$$\mu_t(\omega, H)=v_x/E_x, \tag{1}$$

$$\mu_H(\omega, H)=cE_y/HE_x. \tag{2}$$

$$\mu_{tH}(\omega, H)=v_y/E_y=\mu_t(\omega, H)\{1+[H\mu_H(\omega, H)/c]^2\}^{-1}. \tag{3}$$

Some of the resonances may be illustrated by spherical energy surfaces with a single (relaxation) frequency ν and $\omega_H=qH/m^*c$. We find that μ_t, μ_H, and μ_l are independent of H:

$$\mu_t=\mu_H=\mu_l=q/\{m^*(\nu+i\omega)\}, \tag{4}$$

$$\mu_{tH}=q(\nu+i\omega)/\{m^*[(\nu+i\omega)^2+\omega_H^2]\}, \tag{5}$$

$$\mu_c=q[\nu+i(\pm\omega+\omega_H)]/\{m^*[(\nu+i\omega)^2+\omega_H^2]\}. \tag{6}$$

The plus sign in μ_c holds when the field rotation and cyclotron orbit have the same direction. If $\omega>10\nu$, as may be achieved in Ge at low temperatures, the resonance peaks observed at $\omega_H=\omega^2-\nu^2$ will be within 1 percent of that proper for m^* alone. If ν is a function of $\mathcal{E}$, then the mobility expressions should be based on finding v_x, v_y as functions of E_x and E_y and averaging over the carriers with a weighting factor of $\mathcal{E}$; for a constant mean free path, this will lead to the customary factors of $8/3\pi$, etc. and to a small magnetoresistance in μ_t. This averaging does not affect the conclusion that if $\omega=\omega_H$, μ_c reduces to $\mu_c(0, 0)$ for the wave rotating in the cyclotron direction.

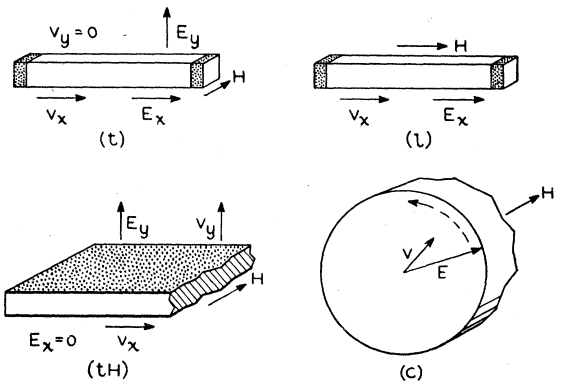

FIG. 1. Some typical situations for observing cyclotron resonances: (t), conventional transverse magnetoresistance configuration; (l), conventional longitudinal magnetoresistance configuration; (tH), a transverse situation in which Hall effect contributes to resistance; (c), circularly polarized electric field.

Herman's calculations[2] suggest that the energy surface for the conduction band in Ge consists of six ellipsoids of revolution lying on [100] directions with a longitudinal mass m_1 and transverse mass m_2. The valence band is probably triply degenerate with surfaces of three sheets of nonellipsoidal shapes.[3] For these sheets we can define "tubes," each having its characteristic mass m_α and corresponding cyclotron frequency.[4]

For an ellipsoidal energy surface given by

$$\mathcal{E}=(P_x^2/2m_x)+(P_y^2/2m_y)+(P_z^2/2m_z) \tag{7}$$

and a magnetic field with direction cosines α, β, λ, the effective cyclotron mass is

$$m^*=[m_xm_ym_z/(m_x\alpha^2+m_y\beta^2+m_z\gamma^2)]^{\frac{1}{2}}. \tag{8}$$

Separate resonances should be observed for each different orientation of ellipsoid to H. Thus, for H parallel to [100] for the six ellipsoids, m^* will equal $(m_1m_2)^{\frac{1}{2}}$ four times and m_2 twice; there will be no longitudinal resonance. For H parallel to [111], $m^*=m_2[3m_1/(m_1+2m_2)]^{\frac{1}{2}}$ six times, and for (l) we find

$$\mu_l=(2m_1+m_2)[(\nu+i\omega)^2+\omega_H^2 9m_1m_2/(2m_1+m_2)(m_1+2m_2)] \div 3m_1m_2(\nu+i\omega)[(\nu+i\omega)^2+\omega_H^2]. \tag{9}$$

Similar, but generally more complex, expressions apply to other cases.

Evidently, if the surfaces are ellipsoids, the determination of the resonance field for several conditions will give a unique determination of the mass parameters and hence of the energy surface shapes.

For the triply degenerate surface, a distribution of masses from zero (at the conical contact of the outer surfaces) to infinity will be present. If the inner surface is nearly spherical, a strong isolated resonance will occur. For this and the doubly degenerate case, it appears likely that the predicted resonance behavior will require difficult numerical calculations. However, it also appears probable that a numerical fit based on the three parameters[3] will be unique.

I am indebted to J. K. Galt, C. Herring, H. Suhl, and R. F. Wick for several stimulating discussions.

[1] Marked electron inertia effects with $\omega/\nu\doteq 0.2$ at 160°K have been reported for electrons in germanium by T. S. Benedict and W. Shockley, Phys. Rev. **89**, 1152 (1953).
[2] F. Herman, Phys. Rev. **88**, 1210 (1952); F. Herman and J. Callaway, Phys. Rev. **89**, 518 (1953).
[3] W. Shockley, Phys. Rev. **78**, 173 (1950).
[4] W. Shockley, Phys. Rev. **79**, 191 (1950).

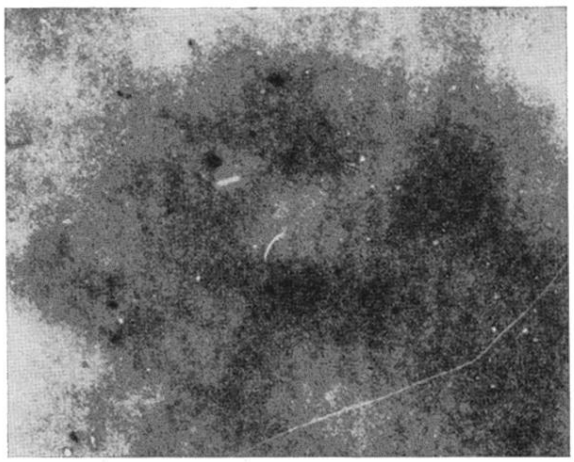

FIG. 1. Electron interference fringes superimposed on uneven crystal background. Total area shown—approximately $3\mu \times 4\mu$; average fringe spacing—1600A.